UCRL- 95835
PREPRINT

CIRCULATION COPY
SUBJECT TO RECALL
IN TWO WEEKS

COMPUTATIONAL ISSUES IN ELECTROMAGNETIC COUPLING TO A SLIT CYLINDER ENCLOSING AN OFF-SET CYLINDER

R. F. Schmucker
R. W. Ziolkowski

This Paper was Prepared for Submittal to
The 1987 ARRAY Conference
Montreal, Canada
April 26-29, 1987

January, 1987

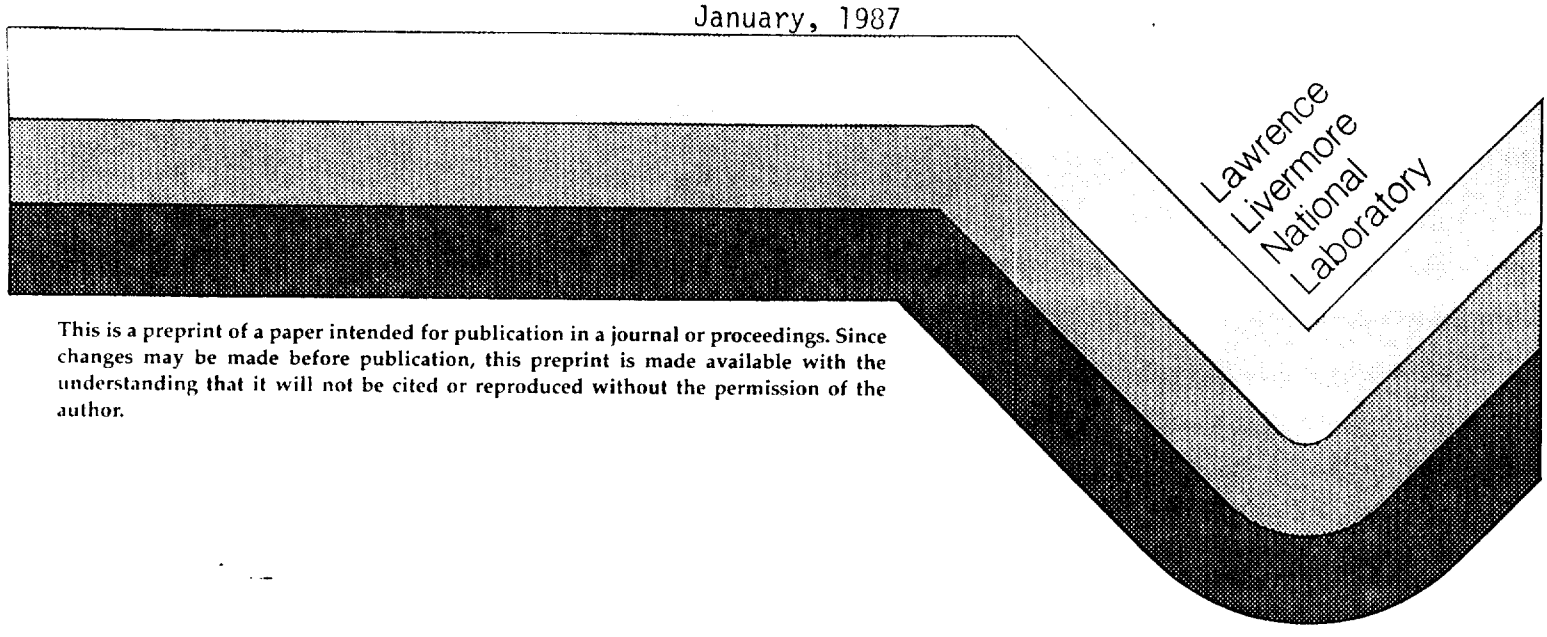

This is a preprint of a paper intended for publication in a journal or proceedings. Since changes may be made before publication, this preprint is made available with the understanding that it will not be cited or reproduced without the permission of the author.

DISCLAIMER

This document was prepared as an account of work sponsored by an agency of the United States Government. Neither the United States Government nor the University of California nor any of their employees, makes any warranty, express or implied, or assumes any legal liability or responsibility for the accuracy, completeness, or usefulness of any information, apparatus, product, or process disclosed, or represents that its use would not infringe privately owned rights. Reference herein to any specific commercial product, process, or service by trade name, trademark, manufacturer, or otherwise, does not necessarily constitute or imply its endorsement, recommendation, or favoring by the United States Government or the University of California. The views and opinions of authors expressed herein do not necessarily state or reflect those of the United States Government or the University of California, and shall not be used for advertising or product endorsement purposes.

Computational Issues in Electromagnetic Coupling to a Slit Cylinder Enclosing an Off-set Cylinder*

Ronald F. Schmucker and Richard W. Ziolkowski

Fields, Materials, Plasmas Modeling Group
Engineering Research Division
Electronics Engineering Department
Lawrence Livermore National Laboratory
Livermore, CA 94550

Abstract

The canonical scattering and aperture coupling problem of a plane wave incident upon a slit cylinder enclosing another off-set cylinder has been analytically solved using a dual series approach. The solution expressions are nested sums involving Bessel functions. Numerical evaluation of the physical quantities of interest (bistatic radar cross sections, induced currents, and induced fields) typically requires Bessel functions for thousands of arguments, and several hundred orders at each argument. Thus, the execution time of the Bessel function routines becomes critical. A comparison of the timing and accuracy of the new FPS Bessel function software with other non FPS Bessel function routines will be given.

In addition, there are two major considerations in developing graphics post-processing routines to display the solutions which result from this modeling. First, there is a large number of different system geometries and incident field conditions to model, each with its own computed solution. Secondly, cross-comparisons of different physical quantities are desired to help develop an understanding of the relevant physics. These post-processing needs have required the development of several new graphics display methods. A variety of examples from this canonical coupling problem will be given to demonstrate the efficacy of these graphical display routines.

Introduction

An analytic solution has been developed for the canonical problem of a plane wave incident on a slit cylinder enclosing an offset interior cylinder. Numerical evaluation of the solution involves the computation of Bessel functions for thousands of arguments and hundreds of orders. Typically, this means approximately one third of the required cpu time used in the computation of a solution for one particular geometry and set of incident field conditions is spent just computing these Bessel functions. Since Bessel functions are well defined, and are of general interest, they are a good candidate for using optimized machine dependant routines. The results of a comparison of the speed and accuracy of two Bessel function packages, one from FPS (X64 architecture only), and another from IMSL (semi machine independent), will be shown.

Another computational issue which is often overlooked in numerical and computational

*This work was performed under the auspices of the U.S. Department of Energy by Lawrence Livermore National Laboratory under contract No. W-7405-Eng-48.

forums is the display of the computed answers. More attention needs to be spent on developing the graphical post-processing portion of computer modeling. This extra emphasis combined with today's more powerful graphics libraries and devices means greatly enhanced comprehension of the results with minor extra effort. These more intuitive displays include: placing drawings on X-Y plots, superimposing contour and halftone pictures, and the simultaneous display of multiple physical quantities. The display of multiple physical quantities is necessary to understand the correlations between them. These techniques have general purpose applicability; graphical examples from this canonical modeling problem will be shown to show their usefulness.

Problem Description

The physical class of problems being explored consists of an electromagnetic plane wave incident upon an infinite slit cylinder enclosing another infinite cylinder (see following diagram).

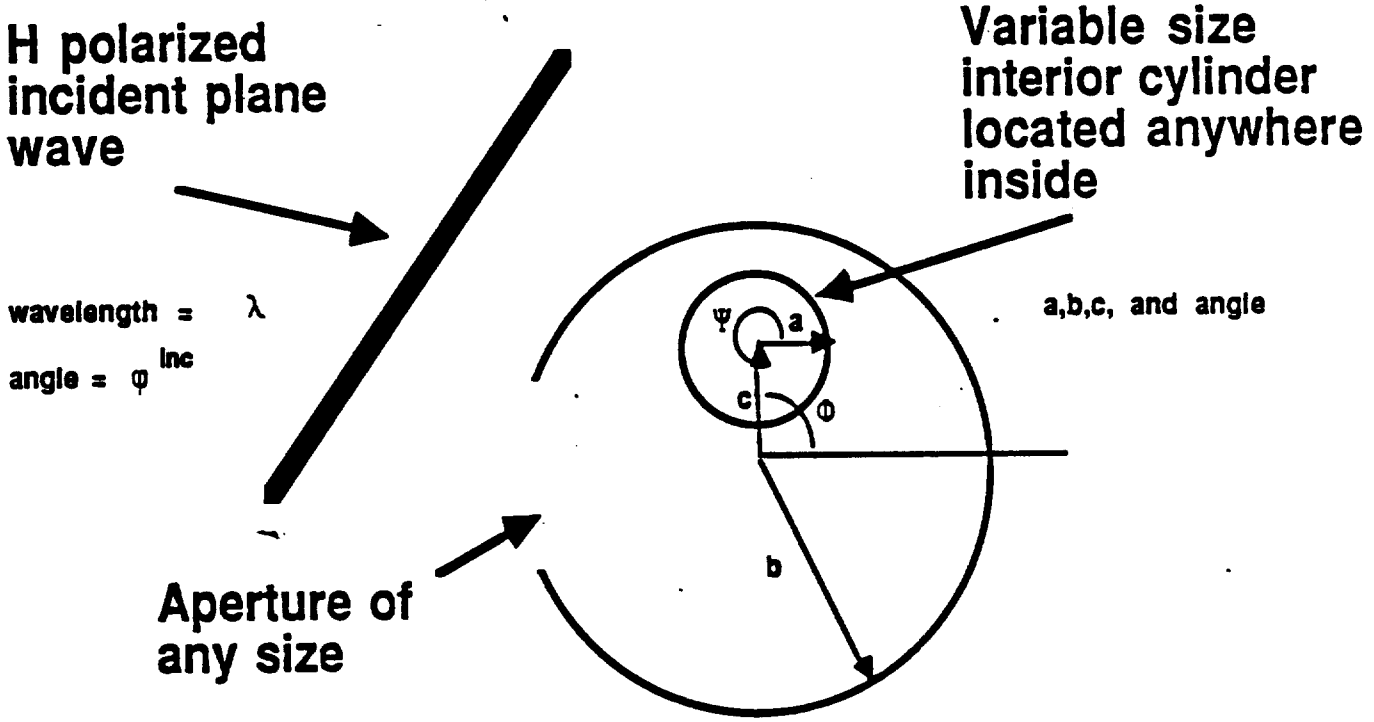

The modal expansions of the field components and the enforcement of electromagnetic boundary conditions produces a system of dual series equations. The first equation applies to the aperture angles, the second equation over the metallic angles. The resulting dual series, which must be solved for the unknown coefficients A_m, is:

$$\sum_{m=-\infty}^{\infty} A_m e^{jm\varphi} = 0$$

$$\sum_{m=-\infty}^{\infty} e^{jm\varphi} \left[A_m J'_m(kb) H'_m(kb) + \sum_{q=-\infty}^{\infty} A_q Y_{mq} H'_m(kb) H'_m(kb) \right] = f(\varphi)$$

where $k=2\pi/\lambda$, z_o is the free space impedance, z is the impedance of the interior cylinder surface, and

$$\Upsilon_{mq} = e^{-j(m-q)\Psi} \sum_{p=-\infty}^{\infty} \Omega_p(ka)\, J_{p-m}(kc)\, J_{p-q}(kc)$$

$$\Omega_p(ka) = -\left[\frac{z J_p(ka) - j z_o J'_p(ka)}{z H_p(ka) - j z_o H'_p(ka)}\right]$$

$$f(\varphi) = -\sum_{q=-\infty}^{\infty} \left[j^q e^{-jq\varphi^{inc}} J'_q(kb) + H'_q(kb) \left[\sum_{p=-\infty}^{\infty} j^p e^{-jp\varphi^{inc}} \Upsilon_{qp} \right] \right] e^{jq\varphi}$$

and $J_n(x)$ is the Bessel function of the first kind of order n. The term $H_n(x)$ is the Hankel function of the second kind, which is defined as $J_n(x) - j\,(Y_n(x))$, where $Y_n(x)$ is the Bessel function of the second kind. The terms $J'_n(x)$ and $H'_n(x)$ are the derivatives of the Bessel and Hankel functions, and are computed using $J_{n\pm1}(x)$ and $H_{n\pm1}(x)$ respectively. The importance of the Bessel function routines can immediately be seen by their frequency of usage in the previous equations. In addition, once the unknown coefficients are determined, the derived expressions for induced electric fields, induced currents, and bistatic (including radar) cross sections are sums involving more Bessel and Hankel function terms. For example, the radial component of the induced electric field contributed by the interior cylinder is:

$$E_{(\text{interior})}(\vec{r}) = \sum_{m=-\infty}^{\infty} B_m e^{jm\Psi} \left[H'_m(k\rho)\sin(\varphi-\Psi) - \left(\frac{jm}{k\rho}\right) H_m(k\rho)\cos(\varphi-\Psi) \right]$$

where ρ is the distance from the interior cylinder to the field point. B_m is itself another summation involving the unknown coefficients A_m, as well as Hankel functions and Bessel functions of the first kind.

Bessel functions

The solution to this coupling problem clearly requires the computation of Bessel functions for numerous arguments. Typically, convergence of the summations requires taking two or three hundred terms, thus two or three hundred orders for each Bessel function argument are needed. The first software implementation used IMSL routines (modified from the Cray version) for the calculation of both $J_n(x)$ and $Y_n(x)$. These IMSL routines provide Bessel functions for integer order and real arguments. Measurement of the cpu intensive portions of the solution code indicated that one third of the cpu time required was spent computing these two Bessel functions. Typically, hours of FPS 264 cpu time are required to completely solve a given set of geometry and incident field conditions. Complete radar cross section scans, which iterate over many wavelengths, can take a FPS-264 cpu day. Therefore one third of the total cpu time is a significant amount of time.

Recently FPS developed some new Bessel function software for their X64 hardware. We applied this new software to try to improve our execution times. Unfortunately, the FPS routines compute the more complicated Bessel functions of integer orders and complex arguments. Since real is a subtype of complex, the FPS software was used and arguments of complex type were passed to it, but with the imaginary part equal to zero. The resulting timings were impressive, especially since the complex Bessel functions are much more difficult to compute. For these real arguments the FPS Bessel function software computed the J and Y Bessel functions in the same time IMSL software computed just the J Bessel function! The accuracy of the two software packages was almost identical. IMSL's software was sometimes capable of squeezing out a few more orders than the FPS software before failing due to machine range limitations.

To further test speed and accuracy, the IMSL routine which computes $J_n(z)$, where z is a complex argument, was also converted to run on the FPS-264. IMSL does not have a routine to compute $Y_n(z)$, so no comparison can be made. Preliminary timing comparisons between the IMSL and the FPS Bessel function software for complex arguments showed drastically varying execution speed ratios depending on the arguments passed. This phenomena was traced to the FPS software having three different algorithms used to compute the Bessel functions. If the absolute value of the imaginary part of the argument is greater than five, one method is used. Otherwise one of two other methods is used, based on the absolute value of the real part of the argument. The domains of the different methods are shown in the following complex plane diagram.

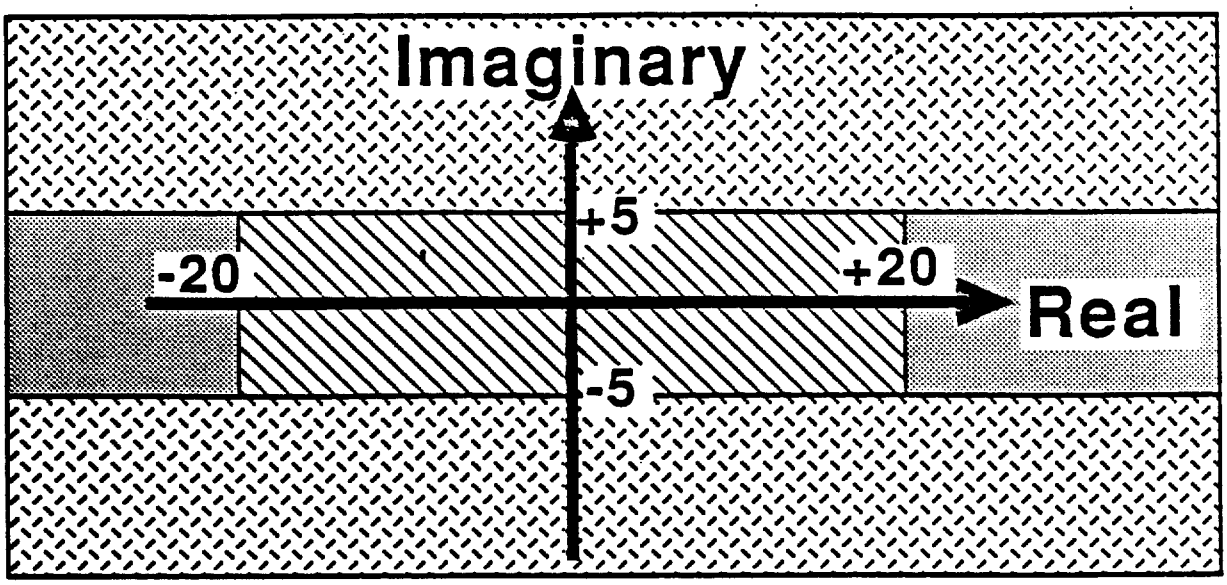

Method 1 used Method 2 used

Method 3 used

The speed of the FPS Bessel function routine is strongly dependent on which domain the arguments of the Bessel function fall in and thus what computational algorithm is used. The following table summarizes the performance of these two Bessel function packages for complex arguments and integer orders.

Bessel function of the first kind, complex argument and integer orders

Method / Argument	Speed $\frac{\text{FPS}}{\text{IMSL}}$	FPS software compared to IMSL software
1 - $\lvert I \rvert > 5.0$	8.3	8.3 X Slower
2 - $\lvert I \rvert < 5.0$ & $\lvert R \rvert < 20.$	0.36	2.7 X Faster
3 - $\lvert I \rvert < 5.0$ & $\lvert R \rvert > 20.$	0.42	2.3 X Faster

As the previous table shows, the FPS Bessel function software will perform between 2.7 times faster and 8.3 times slower than the IMSL software. Clearly, use of this new FPS Bessel function software may help or hurt execution speed, depending on the arguments being computed.

We can solve a large number of canonical problems using this methodology. The choices include various cylinder sizes and placements, different aperture sizes, and different wavelengths and angles of the incidence of the incoming plane wave. To facilitate the understanding of these results (and other problems), the use of graphical displays are important. With the large number of problems to be solved here, and as the complexity of problems being solved on computers increases, conventional techniques are inadequate. Effort should be spent on improving these displays, especially since many of the improvements can be used on a large variety of problems. The following examples will emphasize full utilization of black and white displays. Monochrome devices are more common; and for publications, black and white graphics are preferred.

Many published graphs display their answers on curves but do not include any extra visual clues. It is often relatively easy and extremely helpful to add a supporting picture. The following example adds a diagram of the geometry to the bistatic cross section results.

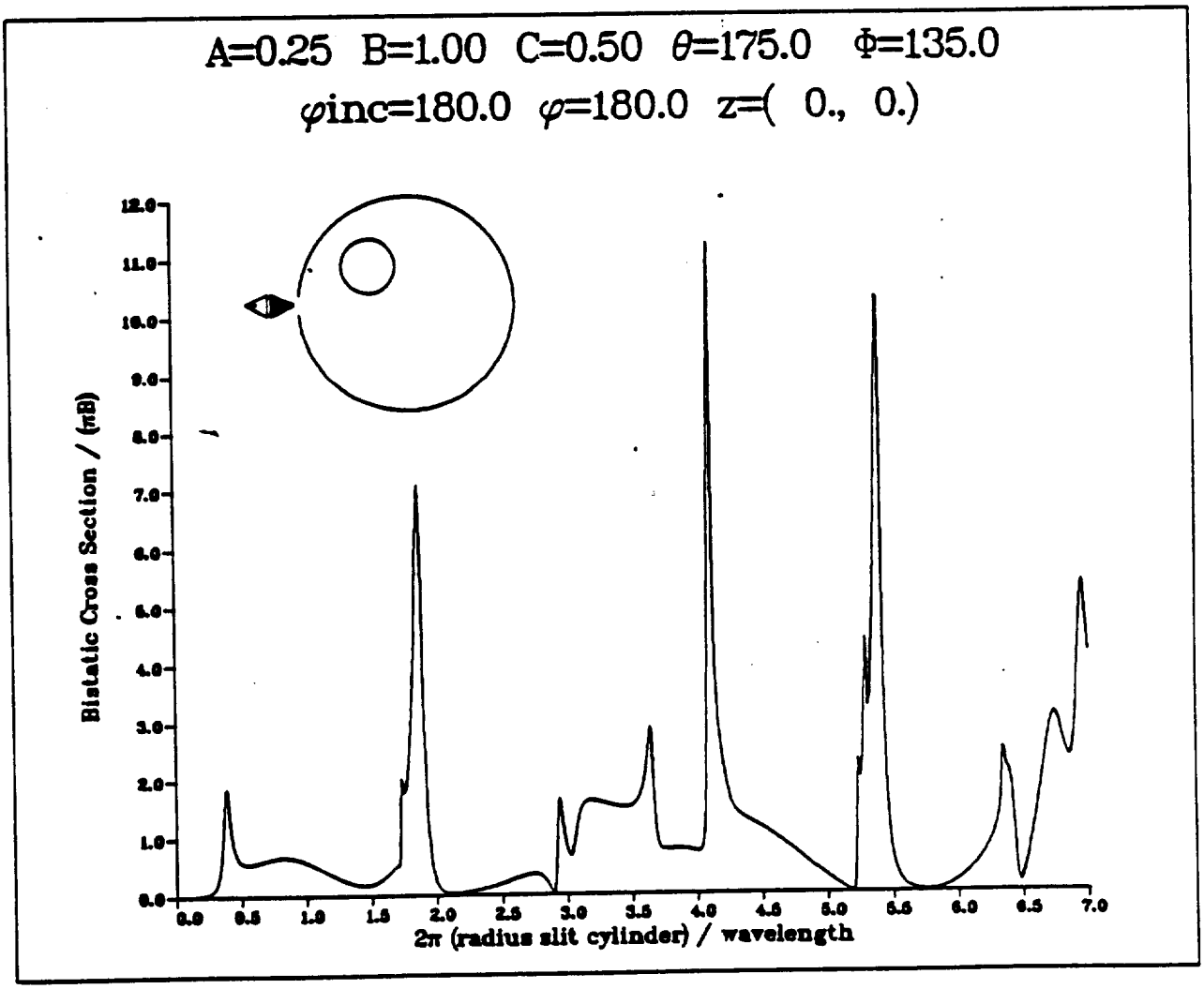

In this diagram the black triangle indicates the direction of the incident energy, and the open triangle depicts the observation angle. Thus, the figure represents a radar cross section result. Once the above notation is known, a glance at this plot provides a description of the problem being solved

and its solution.

The electric fields induced in the interior by the coupling of the incident energy through this cavity backed aperture is another physical quantity of interest. The figure below is the classical contour plot with a diagram of the geometry superimposed.

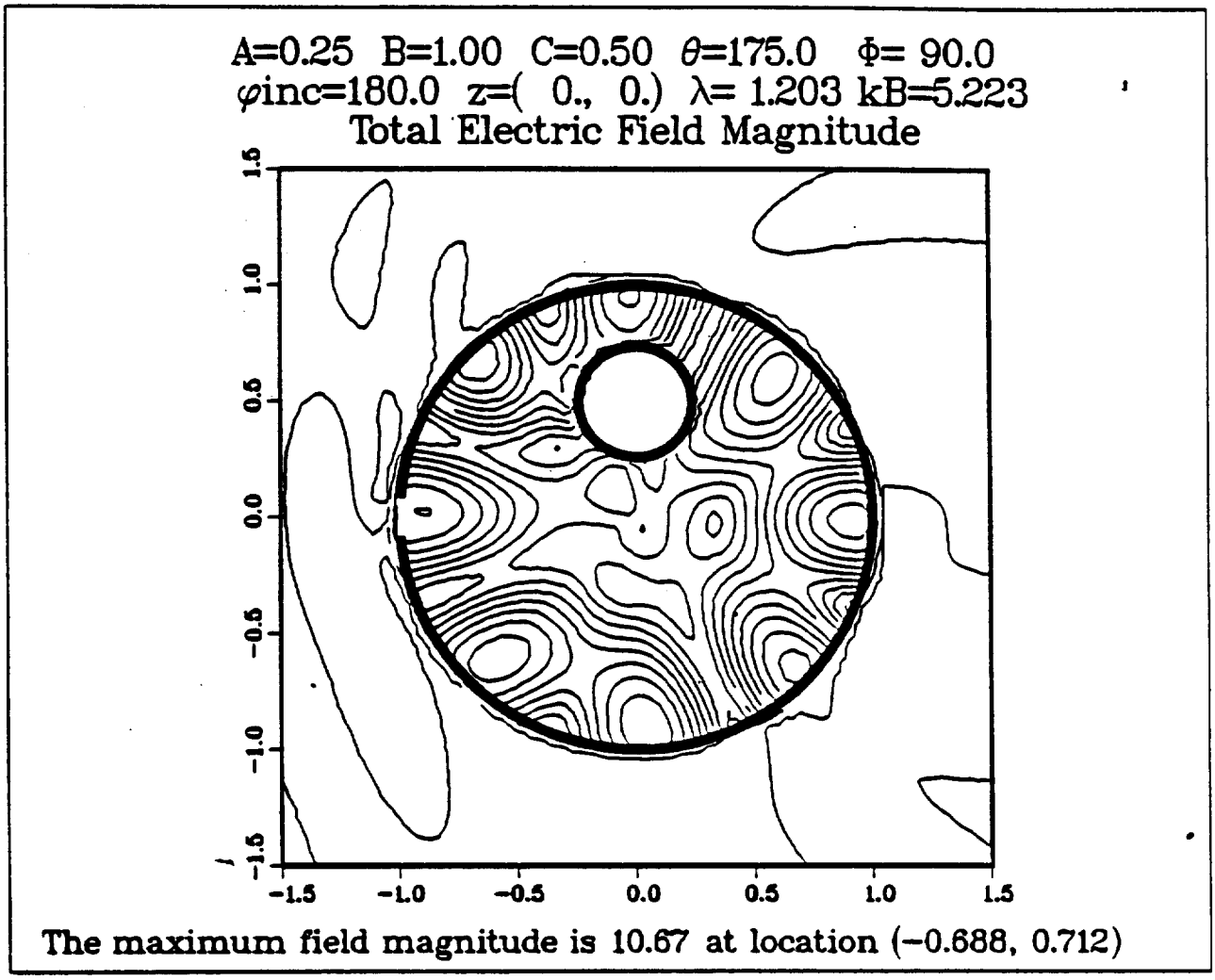

This case represents a situation where the wavelength is resonant with the particular geometry. As one can see, the induced electric field inside this cavity has a great deal of structure. The problem with this display is determining which areas are field enhanced and which areas are suppressed, e.g., is the region near the aperture an increased field area or a null? Labels could be placed on these contour lines; but with the number of field regions in this cavity, reading labels would be tedious if not impossible. Our solution was to superimpose the above contour picture and a simple shaded gray-scale picture. Using darker shading to denote higher field values, this combination produces the following picture.

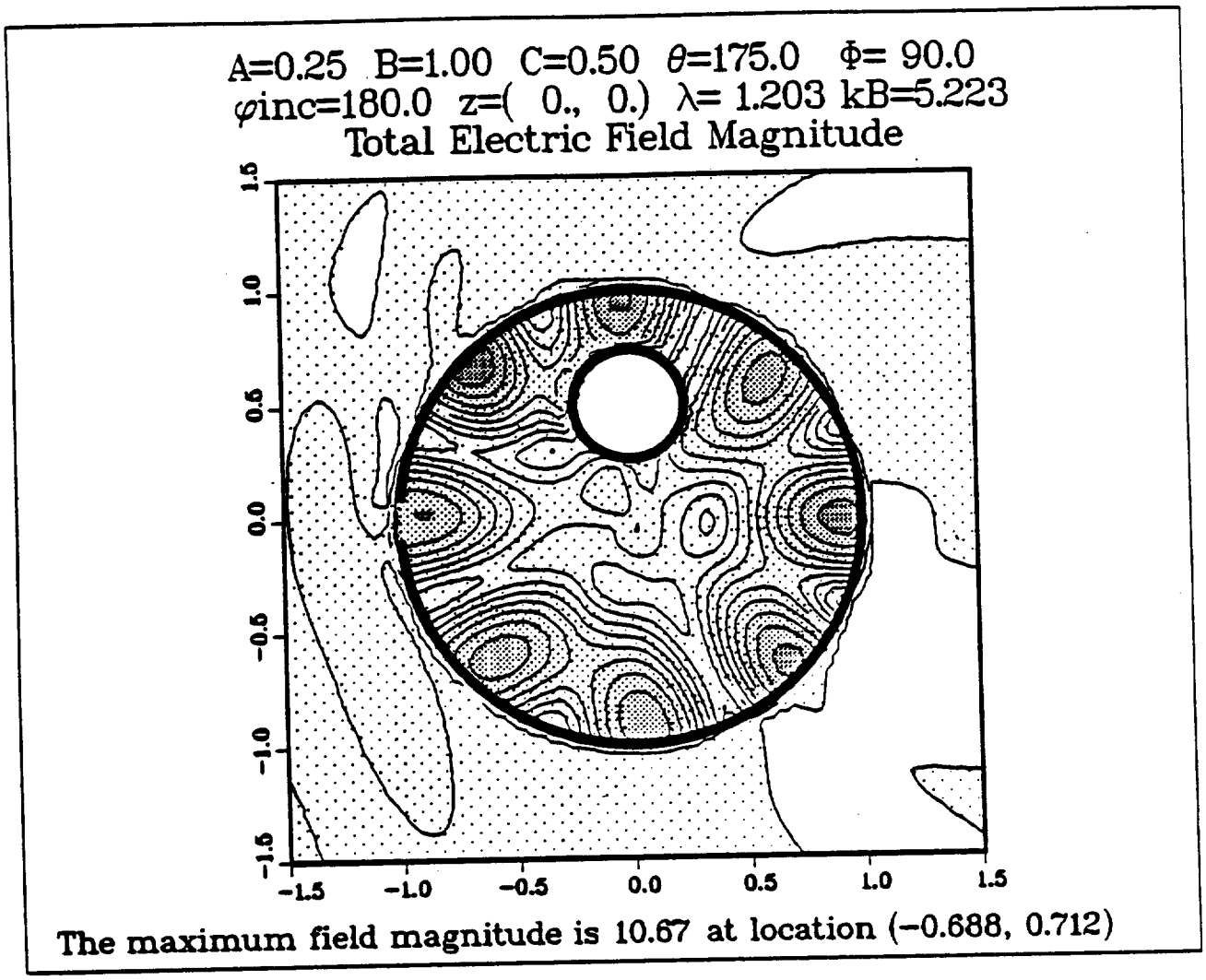

This composite display shows the geometry being solved; the contour levels of the induced electric field; and in an intuitive manner, depicts the magnitudes of the contour levels.

Our display of the currents induced on both the slit cylinder and the interior cylinder also employs some unconventional techniques. The classical method involves simply plotting the magnitude of the induced current versus the angle on the cylinder. This can be done for both the interior cylinder and the slit cylinder. However, to determine how the interior and exterior cylinder currents are correlated, current values from both curves have to be compared. As the wavelength becomes small, the structure of the induced currents becomes complicated, with peak and null points occurring in the induced currents with separation on the order of a few degrees of angle. Thus, it becomes difficult to determine whether a peak in the interior cylinder current aligns with a peak or a null in the slit cylinder current. To remedy this, we have superimposed the current magnitudes for both cylinders in offset polar graphs. The offset is merely the offset of the interior cylinder in the geometry being studied. The current induced on the slit cylinder is plotted as a solid line, while the interior cylinder current is plotted as a dashed line. The ubiquitous geometry diagram is also superimposed to give the following display.

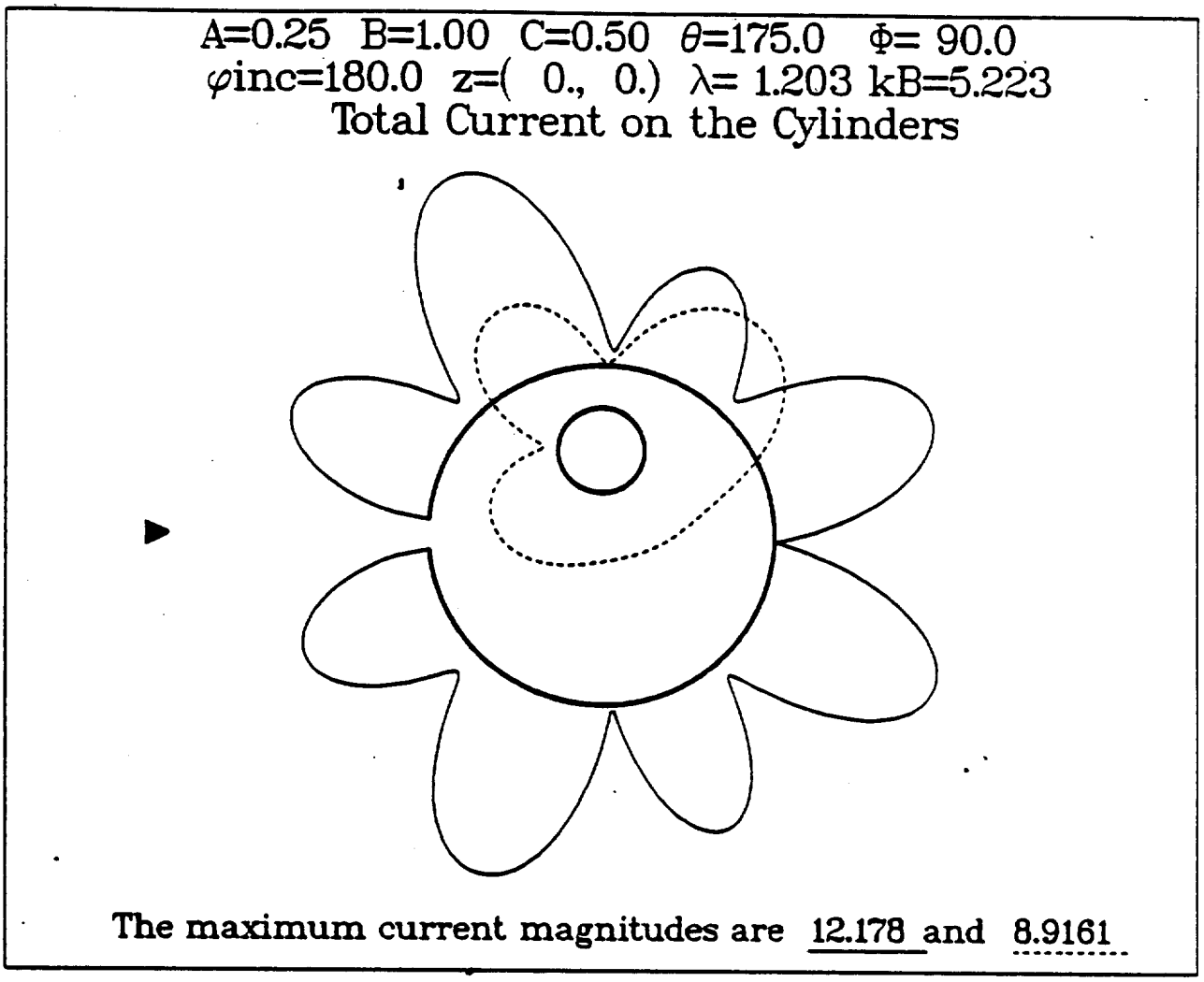

Again, the black triangle depicts the direction of incidence of the incoming plane wave for the particular problem being displayed. This display vastly simplifies the effort required to understand the correlations between the induced current features on both of the cylinders.

There is another overall benefit from putting problem information in the form of a diagram on your plots. The diagram greatly aids in data management, where the sorting and searching of a large quantity of plots can be frustrating and very time consuming. Instead of having to read a selection of parameters off a figure, glancing at the diagram is usually sufficient to identify a particular plot.

Conclusions

The new FPS Bessel function software correctly computes Bessel functions of the first and second kind for complex arguments and integer orders. This FPS software in general executes over twice as fast as software packages not optimized to FPS X64 hardware. However, if only computing Bessel functions of the first kind for complex arguments with the magnitude of the imaginary parts greater than five, the FPS software is exceedingly slow and better alternatives

exist.

The addition of supplementary graphical information to traditional display formats can greatly enhance the clarity of a display. By using some nonstandard techniques, color does not have to be a prerequisite to good graphics. But whether using color or not, improved graphics convey both better understanding and decrease the time required to assimilate results.